

# Constraining Quintessence with the New CMB Data

Michael Doran, Matthew Lilley and Christof Wetterich  
*Institut für Theoretische Physik der Universität Heidelberg  
 Philosophenweg 16, D-69120 Heidelberg, Germany*

The CMB data recently released by BOOMERANG and MAXIMA suggest that the anisotropy spectrum has a third peak in the range  $800 < l_3 < 900$ . A combination of this result with constraints from large-scale structure permit us to differentiate between different quintessence models. In particular, we find that inverse power law models with power  $\alpha > 1$  are disfavoured. Models with more than 5% quintessence before last scattering require a spectral index greater than 1. These constraints are compared with supernovae observations. We also show that the CMB alone now provides strong evidence for an accelerating universe.

PACS numbers: 98.80.-k, 98.80.Es, 98.80.Cq, 95.35.+d

Two independent observations suggest that a significant part of the energy density is homogeneously distributed over the observable Universe: the accelerated expansion [1,2] and the mismatch between the amount of matter in structures and the critical energy density. An accelerated expansion implies that the energy density of the Universe is dominated by a component with negative pressure. The standard negative pressure term, Einstein's cosmological constant, is plagued by enormous fine-tuning problems [3,4], making it seem extremely unnatural. An alternative suggestion for explaining homogeneously-distributed dark energy is quintessence – a scalar field with a slowly-decaying potential [5,6]. Quintessence can lead to a Universe which is accelerating today, without the severe fine-tuning of parameters, or of initial conditions [5–7] (a property referred to as tracking [8]). The field has a time-varying equation of state, becoming dominant only recently thus allowing processes like nucleosynthesis and structure formation to occur unimpeded [6,9]. For a review of quintessence and its properties, see [10] or [11]. There are several different ways of implementing quintessence, generally involving different functional forms for the scalar field action [5,6,12–14], or couplings to matter [15–17]. These different models have common properties, such as tracking and a negative equation of state today, but also differ in their evolution with time. This non-genericity of quintessence makes it difficult to devise observational tests which could detect it and even more difficult to rule it out. Likelihood analysis involving several different types of observation can give good constraints on a given model, but since there is no theoretically-preferred potential we find it more instructive to look for generic, model-independent information. We seek observations sensitive to the amount of dark energy at different epochs in the history of the Universe – in this way the differing time evolution of different quintessence models and a cosmological constant can be compared.

In a recent paper a convenient model-independent framework for quantifying the sensitivity of the Cosmic Microwave Background (CMB) to quintessence was proposed [18] (see also [19]). It was demonstrated that the location of the CMB peaks depend on three dark-energy

related quantities: the amounts of dark energy today  $\Omega_\phi^0$  and at last scattering  $\bar{\Omega}_\phi^{\text{ls}}$  as well as its time-averaged equation of state  $\bar{w}_0$ . In this way, it could be possible to extract information on the amount of quintessence present before last scattering: if  $\bar{\Omega}_\phi^{\text{ls}}$  turns out to be non-zero, we would have strong evidence for non-cosmological constant dark energy. This procedure can also be used to differentiate between different quintessence models. It was emphasized that the acoustic scale  $l_A$  (which is defined below) is a convenient single quantity for characterizing aspects of the CMB, in the way that  $\sigma_8$  (the *rms* mass fluctuation on scales of  $8h^{-1}\text{Mpc}$ ) is used for cluster abundance constraints.

Recent measurements of the CMB [20,21] show three peaks as distinct features, seeming to confirm beyond any reasonable doubt the inflationary picture of structure formation from predominantly adiabatic initial conditions. In this letter we analyse the new data and in particular the consequences of the measured peak locations for quintessence. We find that when combined with constraints from large-scale structure (LSS), models where the scalar field has an inverse-power potential are disfavoured, as are models with more than 5% quintessence before last scattering unless the spectral index  $n > 1$ . We also show that the new CMB data provides strong evidence for an accelerating universe, independent of supernovae (SNe Ia) data, to which we return at the end of this note.

In this work, we have assumed a flat universe, with  $\Omega_b h^2 = 0.022 \pm 0.003$  and  $n = 1$  unless otherwise stated.

The CMB peaks arise from acoustic oscillations of the primeval plasma just before the universe becomes translucent. The angular momentum scale of the oscillations is set by the *acoustic scale*  $l_A$  which for a flat universe is given by

$$l_A = \pi \frac{\tau_0 - \tau_{\text{ls}}}{\bar{c}_s \tau_{\text{ls}}}, \quad (1)$$

where  $\tau_0$  and  $\tau_{\text{ls}}$  are the conformal time today and at last scattering and  $\bar{c}_s$  is the average sound speed before decoupling. The value of  $l_A$  can be calculated simply, and for flat universes is given by [18]

$$l_A = \pi \bar{c}_s^{-1} \left[ \frac{F(\Omega_\phi^0, \bar{w}_0)}{(1 - \bar{\Omega}_\phi^{\text{ls}})^{1/2}} \left\{ \left( a_{\text{ls}} + \frac{\Omega_r^0}{1 - \Omega_\phi^0} \right)^{1/2} - \left( \frac{\Omega_r^0}{1 - \Omega_\phi^0} \right)^{1/2} \right\}^{-1} - 1 \right], \quad (2)$$

with

$$F(\Omega_\phi^0, \bar{w}_0) = \frac{1}{2} \int_0^1 da \left( a + \frac{\Omega_\phi^0}{1 - \Omega_\phi^0} a^{(1-3\bar{w}_0)} + \frac{\Omega_r^0(1-a)}{1 - \Omega_\phi^0} \right)^{-1/2}. \quad (3)$$

Here  $\Omega_r^0, \Omega_\phi^0$  are today's radiation and quintessence components,  $a_{\text{ls}}$  is the scale factor at last scattering (if  $a_0 = 1$ ),  $\bar{c}_s, \bar{\Omega}_\phi^{\text{ls}}$  are the average sound speed and quintessence components before last scattering and  $\bar{w}_0$  is the  $\Omega_\phi$ -weighted equation of state of the Universe ( $w(\tau) = p(\tau)/\rho(\tau)$ )

$$\bar{w}_0 = \int_0^{\tau_0} \Omega_\phi(\tau) w(\tau) d\tau \times \left( \int_0^{\tau_0} \Omega_\phi(\tau) d\tau \right)^{-1}. \quad (4)$$

The location of the peaks is slightly shifted by driving effects and we compensate for this by parameterising the location of the  $m$ -th peak  $l_m$  as in [22,23]

$$l_m \equiv l_A (m - \varphi_m). \quad (5)$$

The reason for this parameterization is that the phase shifts  $\varphi_m$  of the peaks are determined predominantly by pre-recombination physics, and are independent of the geometry of the Universe. The values of the phase shifts are typically in the range  $0.1 \dots 0.5$  and depend on the cosmological parameters  $\Omega_b h^2, n, \bar{\Omega}_\phi^{\text{ls}}$  and the ratio of radiation to matter at last scattering  $r_\star = \rho_r(z_\star)/\rho_m(z_\star)$ . It is not in general possible to derive analytically a relation between the cosmological parameters and the peak shifts, but fitting formulae, describing their dependence on these parameters were given in [23].

It was shown [23] that  $\varphi_3$  is relatively insensitive to cosmological parameters, and that by assuming the constant value  $\varphi_3 = 0.341$  we can estimate  $l_A$  to within one percent if the location of the third peak  $l_3$  is measured, via the relation

$$l_A = \frac{l_3}{3 - \varphi_3}. \quad (6)$$

The measurement of a third peak in the CMB spectrum by BOOMERANG [20] now allows us to extract the acoustic scale  $l_A$  and use this as a constraint on cosmological models. The BOOMERANG team recently performed a model-independent analysis of their data [24], and found the third peak to lie in the region

$$l_3 = 845^{+12}_{-25}, \quad (7)$$

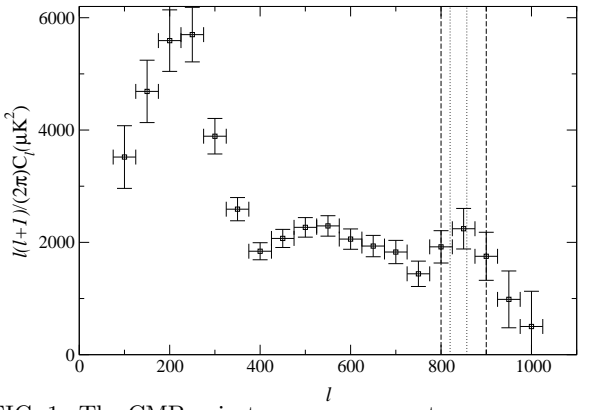


FIG. 1. The CMB anisotropy power spectrum as measured by BOOMERANG [20]. The inner vertical lines show the region  $820 < l_3 < 857$  as calculated by the BOOMERANG team [24], and the outer lines our more conservative region  $800 < l_3 < 900$ .

from which we calculate the value

$$l_A = 316 \pm 8. \quad (8)$$

If we instead chose the more conservative assumption that  $800 < l_3 < 900$ , we would get the bound

$$l_A = 319 \pm 23, \quad (9)$$

We will perform our analysis using both of these ranges for the location of the third peak. The two ranges are displayed, along with the BOOMERANG data, in Fig. 1. Independently of [24] we have performed cubic spline fittings to the data presented in [20], as well as to the combined multiple-experiment data given in [25]. We allowed the data to vary according to the gaussian errors given. We find for the BOOMERANG and combined data respectively:

$$l_1 = 221 \pm 14, \quad 222 \pm 14 \quad (10)$$

$$l_2 = 524 \pm 35, \quad 539 \pm 21 \quad (11)$$

$$l_3 = 850 \pm 28, \quad 851 \pm 31 \quad (12)$$

We applied our CMB-derived  $l_A$  constraints to two types of quintessence model: an inverse power law (IPL) potential [6], given by

$$V(\phi) = V_0 \phi^{-\alpha}, \quad (13)$$

and a 'leaping kinetic term' (LKT) model [14], where the Lagrangian is given by

$$\mathcal{L}(\phi) = \frac{1}{2} (\partial_\mu \phi)^2 k^2(\phi) + M_P^4 \exp(-\phi/M_P), \quad (14)$$

and kinetic term

$$k(\phi) = k_{\text{min}} + \tanh[(\phi - \phi_1)/M_P] + 1, \quad (15)$$

with  $M_P^{-2} = 8\pi G$ . The constants  $V_0$  and  $\phi_1$  determine the value of  $\Omega_\phi$  today in each case. The IPL model has

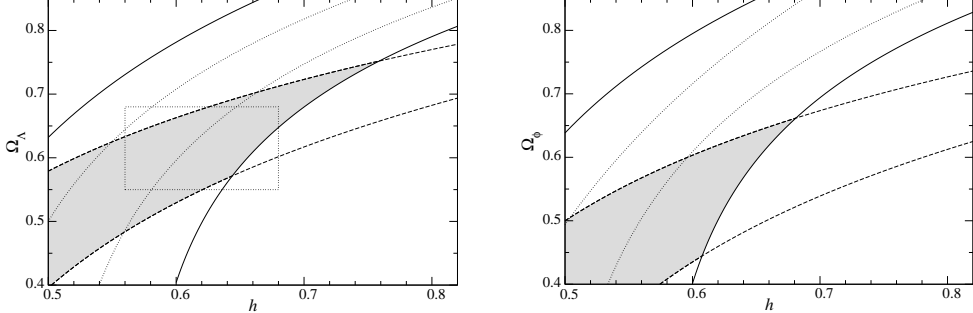


FIG. 2. BOOMERANG (solid lines give conservative bound, dotted lines more strict bound) and LSS (dashed lines) constraints in  $\Omega_\Lambda$ - $h$  plane (left) and  $\Omega_\phi$ - $h$  plane for LKT quintessence with  $\Omega_\phi^{\text{ls}} = 0.05$  (right). The dotted box indicates the 1- $\sigma$  maximum likelihood ranges obtained by the BOOMERANG data analysis team with flatness and LSS priors.

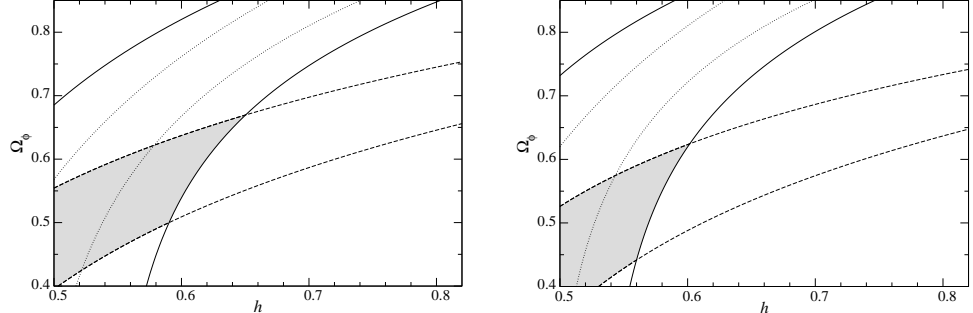


FIG. 3. Constraints in the  $\Omega_\phi$ - $h$  plane for IPL quintessence, from BOOMERANG and LSS,  $\alpha = 1$  (left) and  $\alpha = 2$  (right).

equation of state today given by  $w = -2/(\alpha + 2)$  and in the LKT model the constant  $k_{\min}$  can be tuned to give specific values of  $\bar{\Omega}_\phi^{\text{ls}}$ . In addition, one could multiply the argument of the  $\tanh()$  in Equation (15) by a factor in order to steepen the increase in the kinetic term. The equation of state today,  $w_0 \equiv w(\text{today})$ , depends strongly on the precise shape of  $k(\phi)$ . This is relevant for supernovae observations, and we emphasize that, in general,  $w_0 \neq \bar{w}_0$ . For a steep increase in  $k(\phi)$ , one can have  $w_0$  very close to  $-1$  (see also figure 4). Other models of quintessence share the effective time dependence of  $w$  [26,27].

We also applied the constraints to a cosmological constant ( $\Omega_\phi^0 \equiv \Omega_\Lambda$ ) universe (i.e. IPL quintessence with  $\alpha = 0$ ) for comparison.

In Figs 2, 3 we show for our chosen dark energy models the range of  $\Omega_\phi$  and  $h$  allowed by Equations (8) and (9). These ranges are similar for the cosmological constant, LKT (also for  $\bar{\Omega}_\phi^{\text{ls}} = 0.2$ ) and IPL for small  $\alpha$  whereas IPL with  $\alpha = 2$  would be pushed to small values of  $h$ . The comparatively low values of  $h$  inferred from the BOOMERANG data can be combined with information from LSS formation. The growth of density fluctuations ceases when quintessence starts to dominate. In this way LSS can serve as a probe of quintessence at intermediate redshifts. Cluster abundance constraints for quintessence models with constant equation of state yield [28]

$$\sigma_8 \Omega_m^\gamma = 0.5 - 0.1 [(n - 1) + (h - 0.65)] \quad (16)$$

where  $\gamma$  depends slightly on  $w$ , and typically  $\gamma \sim 0.6$ . In [28], the uncertainty for Equation (16) was estimated as 20% at 2- $\sigma$ , and this is the constraint shown in the plots. We have chosen to shade the 2- $\sigma$  LSS and conservative  $l_A$  concordance region in the  $\Omega_\phi^0$ - $h$  plane, but not to impose any bounds on these parameters. Recently, however, the HST has measured  $h = 72 \pm 8$  [29], and the 2dF survey  $\Omega_m h = 0.20 \pm 0.03$  [30].

The current CMB and LSS data are consistent with a cosmological constant (Fig. 2). The LKT model with 5% quintessence at last scattering is marginally compatible for small  $h$ . If the amount of quintessence at last scattering is increased beyond 5%, the  $l_A$  bounds do not change significantly. Compatibility with LSS data would require, however, even higher  $h$ -values, at odds with the BOOMERANG data. In contrast to the CMB measurements, the determination of  $\sigma_8$  by cluster abundances involves systematic uncertainties that are difficult to quantify. Furthermore, the theoretical expectation for  $\sigma_8$  depends strongly on the spectral index  $n$ . Some inflationary models indeed connect the smallness of primordial density fluctuations to  $n = 1.1 - 1.15$  [31]. Increasing  $n$  increases the amount of dark energy allowed during structure formation. For  $n = 1.1$ , the LKT model with 10% quintessence at last scattering becomes feasible.

The IPL model (Fig. 3) with  $\alpha = 2$  is disfavoured, with higher values of  $\alpha$  even worse, but  $\alpha = 1$  survives.

Of course IPL models with  $\alpha < 1$  provide a better fit to the data, however for  $\alpha \rightarrow 0$  IPL approaches the cos-

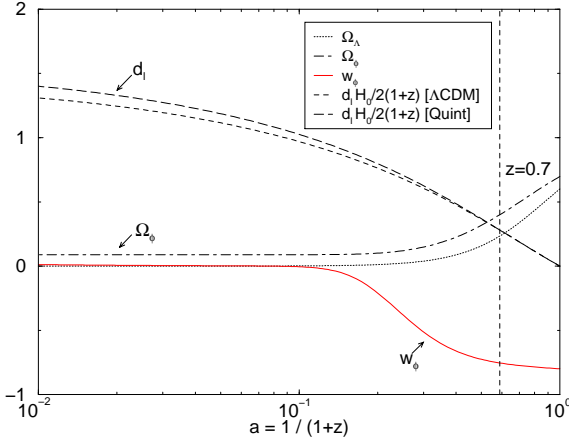


FIG. 4. The luminosity distance  $d_l(z)$  (plotted as  $d_l(z)H_0/2(1+z)$ ) and  $\Omega(z)$  for a  $\Lambda$ CDM and a LKT universe with  $\Omega_\Lambda^0 = 0.6$  and  $\Omega_\phi^0 = 0.7$  respectively. The equation of state  $w_\phi(z)$  of the LKT quintessence is also given. For low redshift, the equation of state is close to  $-1$ ,  $w_0 = -0.8$ . For  $w_0[\Omega_\phi^0]^{1.4} = \Omega_\Lambda^0$ , the luminosity distance of both LKT and  $\Lambda$ CDM fall on top of each other in the redshift region relevant for current SN Ia analysis (two upper most curves). Despite the similar late time behaviour, the LKT model has  $\Omega_\phi \approx 0.1$  from very early times on, whereas in the cosmological constant model, dark energy plays a role only recently.

ological constant and the problem of naturalness becomes more and more severe (with possible exceptions [32]). Similar conclusions on the IPL model have been derived from the old BOOMERANG data [33], but only for fixed  $h = 0.65$ . We see from our figures that the results can be very sensitive to changes in  $h$ .

Other constraints on dark energy come from SN Ia analysis [34–39]. A cosmological constant is restricted to  $\Omega_\Lambda \in [0.5, 0.9]$  at  $2\sigma$  confidence level [1,40]. For quintessence, the bound on  $\Omega_\Lambda$  can easily be translated into one on  $w_0$  and  $\Omega_\phi^0$ . This is due to a degeneracy of the luminosity distance  $d_l(z)$  in  $w_0$  and  $\Omega_\phi^0$ , and the fact that most of the current SNe Ia data is in the redshift range  $z \in [0.35, 0.7]$ . In this range, an approximate linear relation  $d_l(z)H_0/(1+z) = g_0(z) + xg_1(z)$  holds, depending only on the combination  $x \equiv w_0[\Omega_\phi^0]^{1.4}$ . Put another way, any Quintessence model with  $w_0[\Omega_\phi^0]^{1.4} = -\Omega_\Lambda^{1.4}$  is, by current SN Ia data, indistinguishable from the corresponding  $\Lambda$ CDM universe with  $\Omega_\Lambda$  (see also figure 4). From the bounds  $\Omega_\Lambda \in [0.5, 0.9]$ , we get

$$-0.86 [\Omega_\phi^0]^{-1.4} < w_0 < -0.38 [\Omega_\phi^0]^{-1.4}. \quad (17)$$

For the IPL model, this can be translated into  $\Omega_\phi^0 > 0.3(\alpha + 2)^{5/7}$ , i.e. assuming that  $\Omega_\phi^0 < 0.8$ , we have  $\alpha < 1.9$  (see also [37]). This is comparable to our CMB and LSS constraint. On the other hand, LKT models can be consistent with SNe Ia and nevertheless differ substantially from cosmological constant scenarios for the CMB and LSS (see figure 4). For these models, the CMB+LSS

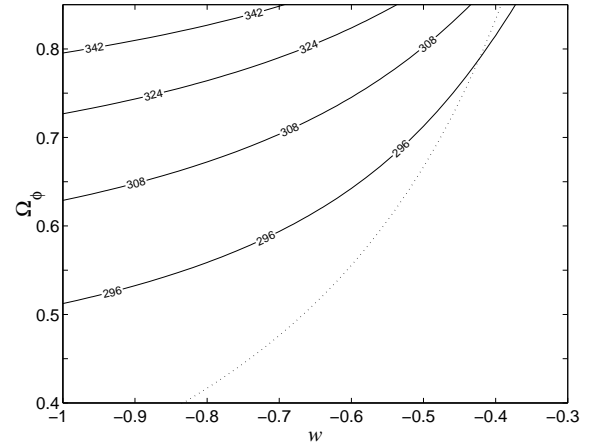


FIG. 5. Lines of constant  $l_A$  in the  $\Omega_\phi^0$ - $w_0$  plane, for  $h = 0.6$ . All universes to the left of the dotted line are accelerating. For larger values of  $h$ , the  $l_A$  lines are shifted north-west.

and the SNe Ia constraints are not directly related and cannot easily be compared.

A flat universe is accelerating today if the dark energy component and its equation of state satisfy

$$\Omega_\phi^0 w_0 < -\frac{1}{3}. \quad (18)$$

Assuming that there is no significant dark energy component at last scattering, we can combine our constraints on  $l_A$  with Equation (2). Fig 5 shows that provided  $h > 0.6$ , the CMB now gives strong evidence for an accelerating universe, independently of supernovae data.

In this letter we have applied the latest CMB data to different models of quintessence, via the easy-to-extract acoustic scale  $l_A$  and combined it with constraints from LSS formation. We have found that inverse power law quintessence models are severely constrained, as are models with more than 5% quintessence at last scattering and spectral index  $n = 1$ . In both cases the models can be compatible with CMB or LSS when taken alone, but not together. In order to use the CMB to *detect* quintessence, via a non-zero density at last scattering, a more accurate measurement of the location of the first CMB peak, and hence the  $\overline{\Omega}_\phi^{\text{ls}}$ -dependent peak shift  $\varphi_1$ , is required.

## ACKNOWLEDGMENTS

We would like to thank L. Amendola, R. Crittenden, B. Mason and J. Schwindt for helpful discussions.

[1] S. Perlmutter *et al.*, *Astrophys. J.* **517** (1999) 565 [[astro-ph/9812133](#)].

[2] A. G. Riess *et al.*, *Astron. J.* **116** (1998) 1009 [[astro-ph/9805201](#)].

[3] Ya. B. Zeldovich, *Pis'ma Zh. Eksp. Teor. Fiz.* **6** (1967) 883 [*JETP Lett.* **6** (1967) 316].

[4] S. Weinberg, *Rev. Mod. Phys.* **61** (1989) 1.

[5] C. Wetterich, *Nucl. Phys. B* **302** (1988) 668.

[6] P. J. Peebles and B. Ratra, *Astrophys. J.* **325** (1988) L17.

[7] E. J. Copeland, A. R. Liddle and D. Wands, *Phys. Rev. D* **57** (1998) 4686 [[gr-qc/9711068](#)].

[8] P. J. Steinhardt, L. Wang and I. Zlatev, *Phys. Rev. D* **59** (1999) 123504 [[astro-ph/9812313](#)].

[9] P. G. Ferreira and M. Joyce, *Phys. Rev. D* **58** (1998) 023503 [[astro-ph/9711102](#)].

[10] L. Wang, R. R. Caldwell, J. P. Ostriker and P. J. Steinhardt, *Astrophys. J.* **530** (2000) 17 [[astro-ph/9901388](#)].

[11] P. Binetruy, *Int. J. Theor. Phys.* **39** (2000) 1859 [[hep-ph/0005037](#)].

[12] K. Coble, S. Dodelson and J. A. Frieman, *Phys. Rev. D* **55** (1997) 1851 [[astro-ph/9608122](#)].

[13] A. Albrecht and C. Skordis, *Phys. Rev. Lett.* **84** (2000) 2076 [[astro-ph/9908085](#)].

[14] A. Hebecker and C. Wetterich, *Phys. Lett. B* **497** (2001) 281 [[hep-ph/0008205](#)].

[15] C. Wetterich, *Astron. and Astrophys.* **301** (1995) 321 [[hep-th/9408025](#)].

[16] L. Amendola and D. Tocchini-Valentini, *Phys. Rev. D* **64** (2001) 043509 [[astro-ph/0011243](#)].

[17] R. Bean, *Phys. Rev. D* **64** (2001) 123516 [[astro-ph/0104464](#)].

[18] M. Doran, M. J. Lilley, J. Schwindt and C. Wetterich, *Astrophys. J.* in press [[astro-ph/0012139](#)].

[19] G. Huey *et al.*, *Phys. Rev. D* **59** (1999) 063005 [[astro-ph/9804285](#)].

[20] C. B. Netterfield *et al.*, [astro-ph/0104460](#).

[21] A. T. Lee *et al.*, *Astrophys. J.* **561** (2001) L1 [[astro-ph/0104459](#)].

[22] W. Hu, M. Fukugita, M. Zaldarriaga and M. Tegmark, *Astrophys. J.* **549** (2001) 669 [[astro-ph/0006436](#)].

[23] M. Doran and M. Lilley, [astro-ph/0104486](#).

[24] P. de Bernardis *et al.*, [astro-ph/0105296](#).

[25] X. Wang, M. Tegmark and M. Zaldarriaga, [astro-ph/0105091](#).

[26] P. Brax and J. Martin, *Phys. Lett. B* **468** (1999) 40 [[astro-ph/9905040](#)].

[27] P. Brax, J. Martin and A. Riazuelo, *Phys. Rev. D* **64** (2001) 083505 [[hep-ph/0104240](#)].

[28] L. Wang and P. J. Steinhardt, *Astrophys. J.* **508** (1998) 483 [[astro-ph/9804015](#)].

[29] W. L. Freedman *et al.*, [astro-ph/0012376](#).

[30] W. J. Percival *et al.*, [astro-ph/0105252](#).

[31] C. Wetterich, *Nucl. Phys. B* **324** (1989) 141.

[32] A. de la Macorra and C. Stephan-Otto, [astro-ph/0106316](#).

[33] A. Balbi *et al.*, *Astrophys. J.* **547** (2001) L89 [[astro-ph/0009432](#)].

[34] S. Perlmutter, M. S. Turner and M. J. White, *Phys. Rev. Lett.* **83** (1999) 670 [[astro-ph/9901052](#)].

[35] D. Huterer and M. S. Turner, *Phys. Rev. D* **64** (2001) 123527 [[astro-ph/0012510](#)].

[36] Y. Wang and P. M. Garnavich, *Astrophys. J.* **552** (2001) 445 [[astro-ph/0101040](#)].

[37] P. S. Corasaniti and E. J. Copeland, [astro-ph/0107378](#).

[38] R. Bean and A. Melchiorri, [astro-ph/0110472](#).

[39] A. de la Macorra and C. Stephan-Otto, [astro-ph/0110460](#).

[40] G. Efstathiou, S. L. Bridle, A. N. Lasenby, M. P. Hobson and R. S. Ellis, [[astro-ph/9812226](#)].